Biophysical Journal Volume 105 October 2013 1581–1589

Elementary Functional Properties of Single HCN2 Channels

S. Thon,[†△] R. Schmauder,[†△] and K. Benndorf[†*]

[†]Institute of Physiology II, University Hospital Jena, Jena, Germany

ABSTRACT Hyperpolarization-activated cyclic-nucleotide-gated (HCN) channels are tetramers that evoke rhythmic electrical activity in specialized neurons and cardiac cells. These channels are activated by hyperpolarizing voltage, and the second messenger cAMP can further enhance the activation. Despite the physiological importance of HCN channels, their elementary functional properties are still unclear. In this study, we expressed homotetrameric HCN2 channels in *Xenopus* oocytes and performed single-channel experiments in patches containing either one or multiple channels. We show that the single-channel conductance is as low as 1.67 pS and that channel activation is a one-step process. We also observed that the time between the hyperpolarizing stimulus and the first channel opening, the first latency, determines the activation process alone. Notably, at maximum hyperpolarization, saturating cAMP drives the channel to open for unusually long periods. In particular, at maximum activation by hyperpolarization and saturating cAMP, the open probability approaches unity. In contrast to other reports, no evidence of interchannel cooperativity was observed. In conclusion, single HCN2 channels operate only with an exceptionally low conductance, and both activating stimuli, voltage and cAMP, exclusively control the open probability.

INTRODUCTION

Electrical rhythmicity in specialized neurons and cardiomyocytes is generated by hyperpolarization-activated cyclic-nucleotide-modulated (HCN) ion channels that generate the current, I_h (I_f, I_q) (1). The channels are composed of four subunits that are encoded in mammals by four related genes, HCN1–HCN4 (2,3). All four types of subunit form functional homotetrameric channels (4–6), but also the formation of multiple heterotetrameric channels has been reported when coexpressing either HCN1 with HCN2 (7,8), HCN1 with HCN4 (9), or HCN2 with HCN4 (10).

HCN channels are primarily activated by hyperpolarizing membrane voltage, thereby opposing the repolarizing phase of the action potential and generating a slow depolarizing pacemaker potential (11). At sympathetic stimulation, the activation of HCN channels is enhanced by the second messenger cAMP. cAMP exerts its action by the binding to a cyclic-nucleotide binding domain (CNBD) included in the C-terminus of each subunit (12). Structurally, whole HCN channels have not been crystallized to date, but tetrameric structures formed by the four C-termini, including the four CNBDs, have been reported for three of the four HCN isoforms (12–14).

The activation gating of HCN channels has been routinely studied in whole cells or in macroscopic patches containing hundreds or thousands of channels. By employing Markovian models, these approaches have shed some light on the interaction of the subunits upon voltage-evoked gating of various HCN channels (15,16). Moreover, in HCN2 channels, cAMP-evoked gating (17) and the reciprocal relationship between the two types of gating (18) have been analyzed. In all Markovian models considered so far, it has been assumed that a channel gates independently of its neighboring channels, that the open probability, P_o, of fully activated channels approaches unity, and that there is only one common opening step of the subunits that is differently recruited depending on the number of subunits already gated by voltage and/or ligand binding.

These assumptions were adopted despite elementary functional properties of HCN channels being controversial. The single-channel conductance was first reported in sinoatrial node cells to be exceptionally small, on the order of 1 pS (19). This low conductance was roughly confirmed by nonstationary noise analysis in pyramidal neurons (20) and by single-channel measurements in multichannel patches of HEK293 cells containing recombinant HCN2 channels (21). In contrast, the respective single-channel conductances were reported to be larger by an order of magnitude, or even more, for recombinant HCN1, HCN2, and HCN4 channels (22), native HCN channels in human atrial myocytes (22), and native channels of rat hippocampus neurons (23).

Furthermore, in HCN2 channels, pronounced cooperativity in the gating between neighboring channels has been reported (21). This result would preclude description of the gating of a single-channel by a Markovian model but would require an adequate inclusion of intermolecular cooperative effects.

In this study, we performed single-channel experiments on homotetrameric HCN2 channels expressed in *Xenopus*

Submitted June 19, 2013, and accepted for publication August 15, 2013.

△S. Thon and R. Schmauder contributed equally to this work.

*Correspondence: Klaus.Benndorf@mti.uni-jena.de

Editor: Cynthia Czajkowski

0006-3495/13/10/1581/9 $2.00

http://dx.doi.org/10.1016/j.bpj.2013.08.027

oocytes in both patches containing one channel and patches containing multiple channels in a sufficiently low number to allow identification of single-channel events. Here, we show that the single-channel conductance is as small as 1.67 pS and that there is no indication of sublevel openings. We also show that cAMP increases the open probability, but not the single-channel current, and that there is no indication for an essential cooperativity between neighboring channels. Hence, HCN2 channels expressed in *Xenopus* oocytes work with a well-defined conductance and as independent molecules with a maximum open probability approximating unity.

MATERIALS AND METHODS

Oocyte preparation and cRNA injection

The surgical removal of oocytes was performed under anesthesia (0.3% 3-aminobenzoic acid ethyl ester) from adult females of *Xenopus laevis*. The oocytes were treated with collagenase A (3 mg/ml; Roche, Grenzach-Wyhlen, Germany) for 105 min in Ca^{2+}-free Barth's solution containing (in mM) 82.5 NaCl, 2 KCl, 1 $MgCl_2$, and 5 Hepes, pH 7.5. After this procedure, oocytes of stages IV and V were manually dissected and injected with ~50 ng of cRNA encoding wild-type mHCN2 channels (NM_008226). After injection with cRNA, the oocytes were cultured at 18°C for 1–3 days in Barth's solution containing (in mM) 84 NaCl, 1 KCl, 2.4 $NaHCO_3$, 0.82 $MgSO_4$, 0.41 $CaCl_2$, 0.33 $Ca(NO3)_2$, 7.5 TRIS, cefuroxim, and penicillin/streptomycin, pH 7.4.

Patch-clamp recording

Currents were recorded with the patch-clamp technique from cell-attached and inside-out patches obtained from *Xenopus* oocytes expressing homotetrameric HCN2 channels of *Mus musculus*. The patch pipettes were pulled (P-2000, Sutter Instrument, Novato, CA) from quartz tubing (Science Products, Hofheim, Germany) with outer and inner diameters of 1.0 and 0.5 mm, respectively. The resistance of the uncoated pipettes was 10–20 MΩ in patches containing 20 or fewer channels and 1.0–1.9 MΩ in macropatches. The bath solution contained (in mM) 100 KCl, 10 EGTA, and 10 Hepes, pH 7.2, and the pipette solution contained (in mM) 120 KCl, 10 Hepes, and 1.0 $CaCl_2$, pH 7.2. For parts of the experiments, 10 μM cAMP (Sigma-Aldrich, St. Louis, MO) or 50 μM ZD7288 (Sigma-Aldrich) were applied with the bath solution.

Currents were recorded at room temperature (18–20°C) with an Axopatch 200B amplifier (Axon Instruments, Foster City, CA). To minimize the rundown typical for HCN channels in inside-out patches (19,24,25), the measurements were started 210 s after the patch excision. Stimulation and data recording were performed with the ISO3 hard- and software (MFK, Niedernhausen, Germany). The sampling rate was 4 kHz and the on-line filter (four-pole Bessel) was set to 1 kHz. If not otherwise noted, the hyperpolarizing pulses lasted 7 s and the time between two pulses lasted 7 s.

Data analysis

Because of the absence of null traces and subtle changes in both the capacitive transient and the leak current, the detection and idealization of single-channel events was not performed by standard threshold techniques but locally from the raw data by an in-house algorithm (IgorPRO, Wavemetrics, Lake Oswego, OR). To this end, the difference between the averages of 11 data points before and after each sampling point was calculated, local maxima or minima were determined, and two thresholds were set (threshold for inclusion, typically 150 fA, and threshold for exclusion to remove artifacts, 700 fA). Events lasting for only one sampling interval (250 μs) were generally ignored to avoid artifacts. In addition, each individual event was verified by eye. The channel number in a patch, N, was obtained from the highest number of unitary steps within a trace of 7 s duration at –130 mV and in the presence of 10 μM cAMP. Some data (see Figs. 1 *A*, 3 *C*, and 5 *A*) were refiltered to 0.1 kHz for display.

Fits were performed by IgorPRO (Wavemetrics).

For a given channel number in a multichannel patch, the 95% confidence intervals of $P_o(t)$ were plotted as the interval between the 0.025 and 0.975 amplitude of the cumulative distribution function of a binomial distribution (N, $P_o(t)$). These intervals were estimated using a β function, as implemented in the Betainv function of Excel (Microsoft, Seattle WA).

The experimental data are given as the mean ± SE. The errors obtained by the fits are given as the SD.

RESULTS

Amplitude of single-channel currents

By using pipettes with a resistance of 10–20 MΩ, we obtained a reasonable number of sufficiently stable patches containing one channel (henceforth referred to as single-channel; Table 1) and patches containing multiple channels. In multichannel traces containing between 2 and 12 channels, there was no evidence for a preferential number of channels in the patch.

First, we considered time courses of activation in multichannel patches containing only a few channels (Fig. 1 *A*) to prove that the recordings with clearly resolved unitary steps of ~200 fA produce activation time courses typical for macroscopic HCN2 currents (Fig. 1 *B*). We measured these time courses for cell-attached conditions, inside-out conditions, and inside-out conditions in the presence of 10 μM cAMP, a saturating ligand concentration. As a result, activation in multichannel patches containing only a few channels was slower and less complete in the inside-out than in the cell-attached configuration, whereas addition of cAMP approximately restored performance to

TABLE 1 Overview of data for single HCN2 channels

	Voltage (mV)	No. of traces	No. of patches	i (fA)	P_o after 7 s	Median of first latency (s)
Cell-attached	−90	14	11	150 ± 13	0.36 ± 0.13	2.22
	−110	24	13	197 ± 5	0.92 ± 0.06	1.46
	−130	45	13	238 ± 6	0.98 ± 0.02	0.40
	−150	13	9	257 ± 9	1	0.30
Inside-out	−90	30	5	—	0	—
	−110	42	7	190 ± 8	0.24 ± 0.07	1.82
	−130	66	7	218 ± 5	0.91 ± 0.04	0.78
	−150	32	5	253 ± 7	0.94 ± 0.04	0.50
Inside-out + cAMP	−90	26	5	165 ± 13	0.15 ± 0.07	1.28
	−110	27	7	197 ± 6	1	0.64
	−130	53	7	216 ± 6	0.98 ± 0.02	0.28
	−150	24	4	249 ± 10	1	0.32

i and P_o denote the amplitude of the single-channel current and the open probability, respectively.

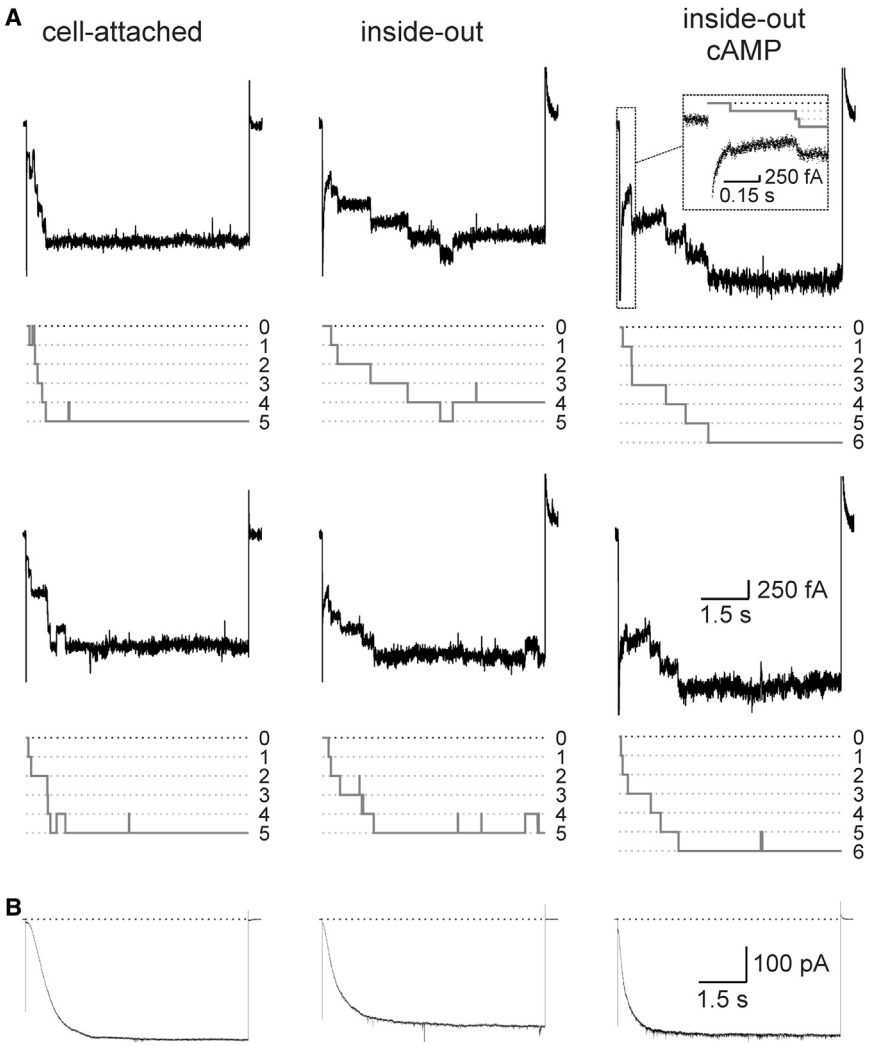

FIGURE 1 Time course of activation generated by HCN2 channels. (*A*) Time courses from multichannel patches in response to a voltage step from 0 mV to −130 mV in the cell-attached, inside-out, and inside-out plus 10 μM cAMP configurations. The two traces at each condition were obtained from the same patch. In the cell-attached and inside-out recordings, the patch contained five channels, whereas in the inside-out recording with cAMP, the patch contained six channels. The idealized traces for the recordings are shown in gray. (*Inset*) Initial time courses at an expanded timescale filtered online at 1 kHz. (*B*) Respective time courses of activation in macropatches containing ~1500 channels.

the cell-attached level. Moreover, currents from multichannel patches containing only a few channels are largely similar to the respective time courses of macroscopic currents, indicating that the channels generating ~200 fA current steps are HCN2 channels.

To clarify whether these unitary steps are full or sublevel openings, and to kinetically characterize the channel activity in more detail, we performed single-channel measurements (Fig. 2). In the cell-attached configuration, the result was that after a variable latency, the channel open times were long, lasting until the end of the 7 s pulse, interrupted sporadically by closing events. The cumulative idealized trace (Fig. 2, *bottom*) shows that the channel is mostly open at the end of the pulse. In the inside-out configuration, activation was slowed and the incidence of closed-channel sojourns was increased, resulting in an idealized cumulative current trace of lower relative amplitude. Hence, at the end of the pulse, the open probability, P_o, was smaller than under cell-attached conditions. Finally, when cAMP was added, the activation kinetics became accelerated and the maximum P_o increased again. These results are consistent with the idea that there is a relevant cytosolic cAMP level in the oocyte (26). Our results also show that a single current level dominates the channel activity, i.e., the channel is activated by a single step from closed to open (462 transitions) and also deactivates by a single step from open to closed (178 transitions). In other words, sublevel openings were not observed in the resolution of our measurements.

Next, we determined the single-channel conductance. We measured the amplitude of single-channel currents, (*i*), at the voltages −90, −110, −130, and −150 mV by local amplitude histograms (Fig. 3 *A*). The respective means (Table 1) were plotted as a function of voltage and the data points at each condition were fitted with a linear function (Fig. 3 *B*). The intercept with the voltage axis was set to the theoretical reversal potential of 4.6 mV, as given by the Nernst equation with $[K^+]_i/[K^+]_o = 0.83$. The result was that the single-channel conductance was indistinguishable for the three patch conditions, yielding a total value of 1.67 ± 0.13 pS. This shows that cAMP exerts an exclusive

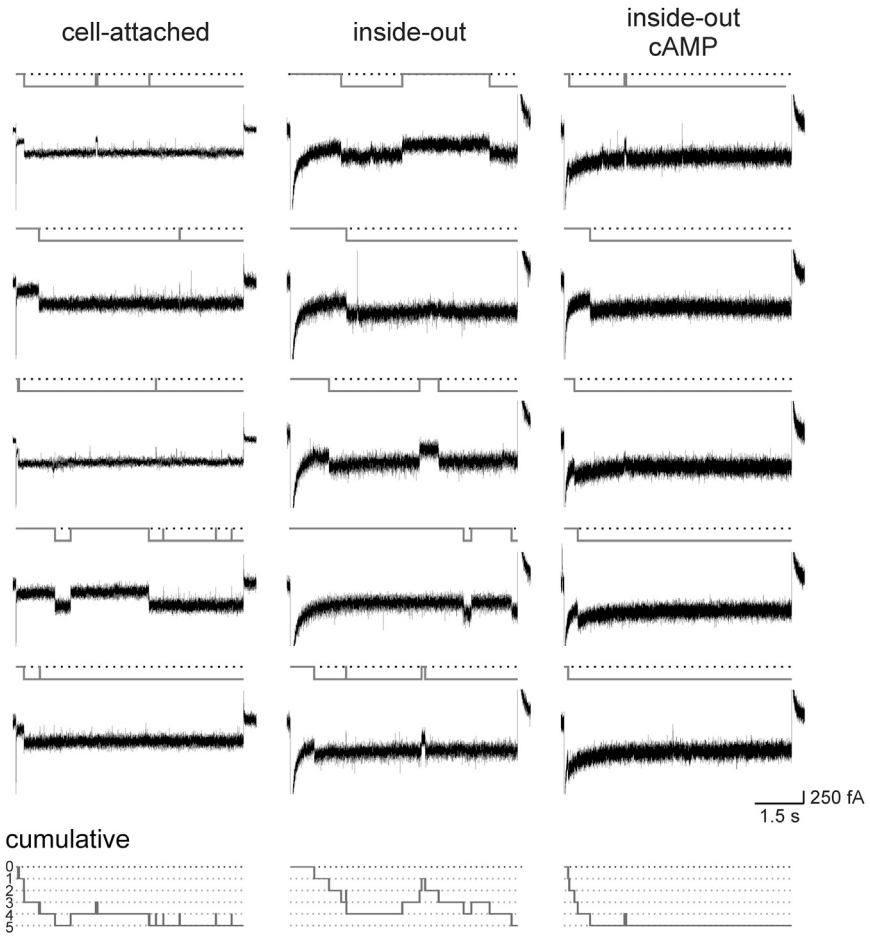

FIGURE 2 Single-channel recordings of HCN2 channels in patches containing one channel at three conditions. The test voltage was −130 mV. The traces in the cell-attached configuration were obtained from two patches, whereas those in the inside-out and inside-out plus cAMP configurations were obtained from one patch. The idealized traces are shown in gray. The closed state is indicated by the black dotted line. The time courses of the cumulative idealized traces (*bottom row*), obtained as the sum of the respective idealized traces above, correspond to the respective time courses in Fig. 1, *A* and *B*.

effect on the channel gating, promoting channel opening by accelerating activation and increasing P_o.

To further confirm that it is indeed HCN2 channels that evoke the 1.67 pS conductance, we applied ZD7288 to patches developing multichannel activity with resolved unitary events (Fig. 3 *C*). ZD7288 is a specific blocker of HCN channel currents (27,28). The result was that 50 μM ZD7288 blocked a major fraction of the current and that the blocking effect was fully reversible after removal of ZD7288 ($n = 3$). The channel blockage of 60% approximately matches earlier results (27). Taken together, these results show that with our solutions, HCN2 channels have a unitary conductance of 1.67 pS, that the channels switch only between one nonconducting and one conducting state, and that cAMP stabilizes this open state.

Kinetics of single-channel activity

To quantify the activation kinetics in single-channel patches, we plotted P_o as a function of time, ($P_o(t)$), at voltages of −90, −110, −130, and −150 mV for the three patch configurations (Fig. 4 *A*). The numbers of patches and traces used are specified in Table 1. In the cell-attached configuration, between −90 and −130 mV, there is a strong effect of voltage on both the activation speed and late activation at the end of the 7 s pulse. In contrast, the trace at −150 mV is similar to that at −130 mV, indicating that the voltage effect saturates at −130 mV. In the inside-out configuration, the activation shifts to more hyperpolarized voltages, resulting in the absence of relevant current activity at −90 mV and a noticeable difference of the traces at −130 and −150 mV. Finally, the effect of the patch excision is reversed by applying 10 μM cAMP.

Next, we studied the first latency, i.e., the time interval between the hyperpolarizing voltage step and the first opening of the channel, from the same primary data. These first latencies were cumulative and normalized with respect to the total number of traces recorded at each condition, thereby including traces without openings. These normalized time courses, which differ from the time courses of P_o by excluding all closures after the channel has once opened, were plotted as a function of time (Fig. 4 *B*). The result for all experimental conditions is that the time courses of the cumulative first latency closely resemble those of the P_o, indicating that subsequent channel closures are of minor importance for the total channel activity. In other words, the activation time course is governed predominantly by the first latency. The median

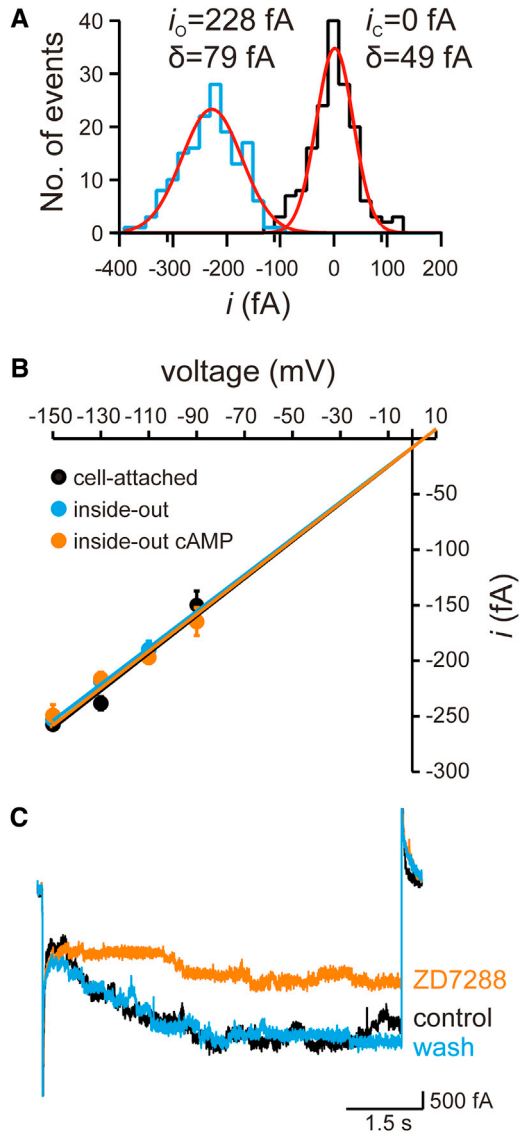

FIGURE 3 Single-channel conductance and block of HCN2 channels. (*A*) Local amplitude histogram for a single-channel opening in an inside-out patch at −130 mV. The histogram was obtained from 160 sampling points immediately before opening (closed state, *black*) as well as after opening (open state, *blue*). The histograms were fitted with two independent Gaussian functions (*red*). The fit parameters for the means, i_x, and widths, σ_x, are $i_o = -228 \pm 1$ fA, $\sigma_o = 79 \pm 2$ fA, $i_c = 0 \pm 1$ fA, and $\sigma_c = 49 \pm 1$ fA. (*B*) Single-channel conductance. The conductance was determined for the three indicated conditions by a linear fit of the respective data points. The single-channel conductance was 1.69 ± 0.12 pS in the cell-attached configuration, 1.64 ± 0.13 pS in the inside-out configuration, and 1.67 ± 0.14 pS in the inside-out configuration with cAMP. The reversal potential of 4.6 mV was set according to the Nernst equation by inserting K^+ concentrations at both sides of the membrane (see text). (*C*) HCN2 channel activity was reversibly blocked by 50 μM ZD7288 in a multichannel patch at −130 mV.

values of the first latencies at all conditions are shown in Table 1.

To further confirm this, we recorded the activity of single channels with longer pulses lasting 25 s. The representative traces recorded at −110 and −130 mV indeed show extremely long openings (Fig. 5 *A*). Because at −110 mV and more negative voltages channel closure appeared regularly only after depolarizing the membrane and open times were generally limited by the experimental protocol rather than the channel dynamics, an adequate open-time analysis could not be performed.

In contrast, most of the closed events, defined by the dwell time between channel closure and reopening, were shorter than the observation time. This led us to perform statistical analysis at the voltage of −130 mV for our three experimental conditions. Due to the limited number of events, we preferred to build cumulative histograms of the closed times (Fig. 5 *B*). In the cell-attached configuration (*black line*), a short component on the order of 10 ms dominated the histogram (>80%). It should be noted, that this fast component is most likely underestimated due to missed brief events. In contrast, in the inside-out configuration, a slow component became prominent in the histograms (*blue line*). Fitting the latter histogram with the double-exponential function,

$$I = 1 - A\exp\left(\frac{-t}{\tau_f}\right) - (1-A)\exp\left(\frac{-t}{\tau_s}\right), \qquad (1)$$

yielded a fast component, $A = 0.36 \pm 0.02$, with a fast time constant of $\tau_f = 12 \pm 1$ ms and a slow component, $(1-A) = 0.64$, with a slow time constant of $\tau_s = 1500 \pm 100$ ms (*red line*). When saturating cAMP was added to the inside-out patches, the cumulative histogram of the closed time (*orange line*) approximated that obtained in the cell-attached configuration (*black line*); both of these conditions are characterized by a fast component. This suggests that cAMP increases the mean current amplitude by reducing the probability of long channel closures and, moreover, that the cytosolic cAMP concentration in the intact oocyte is in the micromolar range.

HCN2 channels gate independently of each other

The data set of patches containing only a single channel enabled us to construct a mean time course of activation for channels that are activated in an unequivocally independent fashion, i.e., in the absence of any cooperative effects between neighboring channels. The black lines in Fig. 6 show these single-channel time courses in terms of $P_o(t)$. It is then possible to compare normalized activation time courses recorded in multichannel patches (*colored lines*) with the activation time course constructed from single-channel patches (*black line*). A pronounced cooperative effect between the channels should cause a deviation of the multichannel traces from the single-channel $P_o(t)$. Assuming a multichannel patch of N independent channels, the number of open channels at each time, t, should follow a binomial distribution, given by $P_o(t)$ and N. We therefore

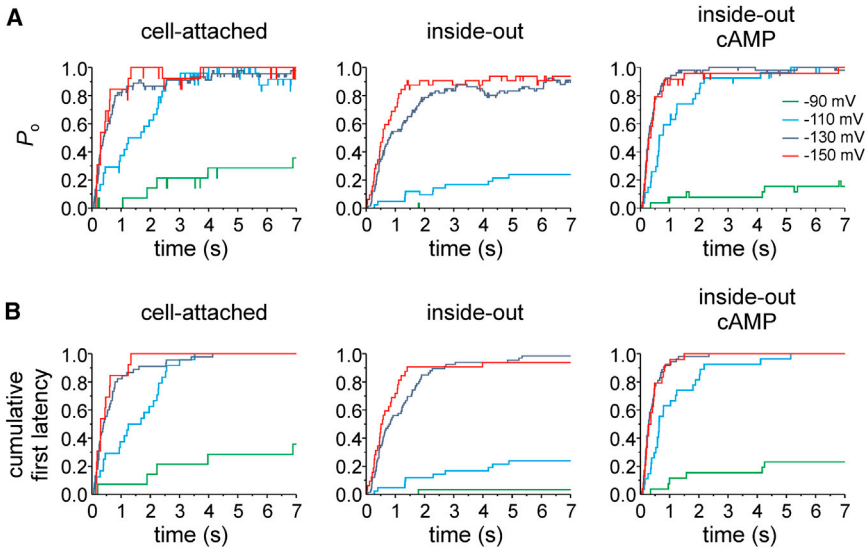

FIGURE 4 Comparison of the time-dependent open probability, P_o, and first latency of HCN2 channel currents obtained from single-channel patches. (*A*) Averaged idealized time courses. (*B*) Cumulative first latencies normalized to the number of traces recorded under the respective conditions, including the traces with no openings within the time window of 7 s.

compared the $P_o(t)$ from single-channel patches with the $P_o(t)$ from multichannel patches using the 95% confidence interval (see Materials and Methods; Fig. 6, *gray areas*). The result is that there was no systematic deviation of the multichannel traces outside the 95% confidence interval. Hence, there is no indication of a relevant cooperative gating of HCN2 channels in multichannel patches as considered herein.

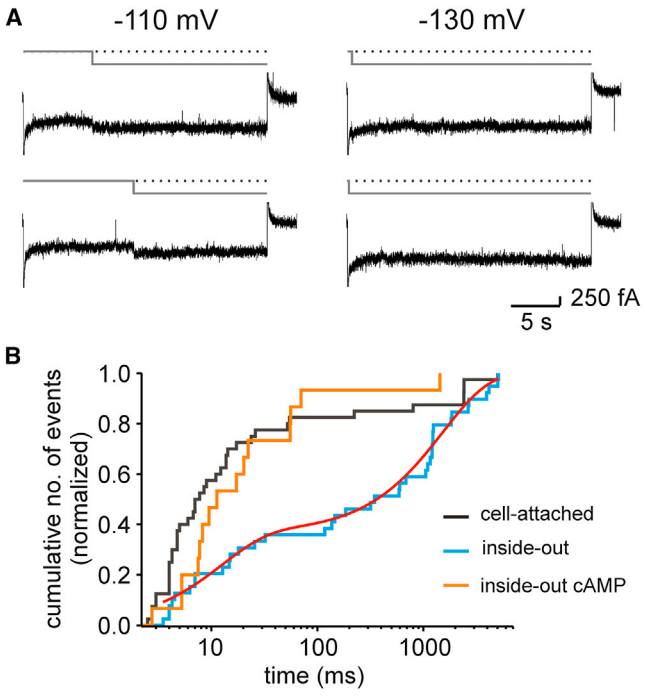

FIGURE 5 Open and closed times of HCN2 channels. (*A*) Selected traces with single-channel activity elicited by pulses of 25 s duration to either −110 or −130 mV. Idealizations of the recordings are shown in gray. Dotted lines represent the closed state. After a channel has once opened, it usually stays open for many seconds. (*B*) Cumulative closed-time histograms for the cell-attached, inside-out, and inside-out plus cAMP configurations at −130 mV. The histogram for the inside-out configuration was fitted by Eq. 1, yielding for the fast component $A_f = 0.36 \pm 0.02$ and $\tau_f = 12 \pm 1$ ms and for the slow component (1-A) = 0.64 and $\tau_s = 1500 \pm 100$ ms.

DISCUSSION

In this study of single HCN2 channels, we showed that the unitary conductance is exceptionally small, that channel opening proceeds by a single step to the only open level, that cAMP increases the open probability but not the single-channel current, and that the open probability of the fully activated channel approximates unity. This was achieved by analyzing the single-channel activity in both single-channel patches and multichannel patches with distinguishable single-channel events.

Our data further suggest that the individual channels in multichannel patches work independently, without cooperative effects between them. These results are of importance for the basic understanding of the HCN2 function and for any interpretation of the gating of these channels in terms of kinetic models. The results also show that HCN2 channels share basic properties with the majority of other channels to generate one dominating single-channel conductance and to gate independently of their neighbor channels of the same type.

Single-channel conductance is exceptionally small

The single-channel conductance of 1.67 pS clearly supports earlier results showing an exceptionally low conductance of 1 pS in sinoatrial node cells (19,29) and 0.68 pS in pyramidal neurons (20). A conductance of 1.65 pS has been reported for recombinant HCN2 channels expressed in HEK 293 cells (21). Very recently, using GFP-labeled channels and patch-clamp fluorometry, Su et al. (30) reported a

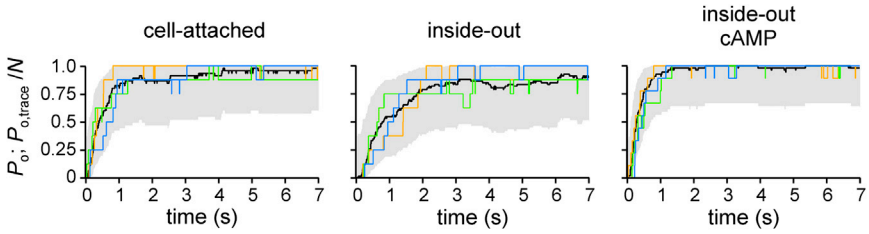

FIGURE 6 Comparison of the time course of activation at −130 mV between channels operating in patches containing only one channel and channels operating in multichannel patches. Plotted are $P_o(t)$ obtained from single-channel patches (*black curves*) and normalized idealized graphs from multichannel patches (*colored curves*). For each condition, three representative multichannel traces are shown. The 95% confidence intervals along $P_o(t)$ are shown in gray. For further explanation, see text.

similarly low value of 1.82 pS using an optical approach. In addition the agreement of our conductance with these values reported in the literature, our results also show that the single-channel conductance is not affected by the binding of cAMP.

The difference between the conductance of recombinant HCN2 channels and that of the native channels is possibly caused by the fact that the molecular nature of the wild-type channels is unknown, leaving open the possibility that they are heterotetrameric. Though a single-channel conductance of 1.67 pS is small and its measurement is challenging, our results are unequivocal. Our measurements do not provide any evidence for a significantly larger single-channel conductance; in particular, no conductance of 19.0 pS or 34.6 pS was observed (22). We also did not observe a conductance of 9.7 pS (23). The reason for these discrepancies remains unclear. In particular, the large conductance values reported by Michels and co-workers (22,31) seem to be less well substantiated, because the authors did not show the typically slow activation time courses for their single-channel activity. In contrast, for the single-channel currents in rat hippocampus neurons these slow time courses were demonstrated (23). Moreover, the authors also report that external Cs^+ ions (32,33) and the specific blocker of HCN channels, ZD7288 (34,35), are effective to block these channels. This raises the questions of whether some of the HCN isoforms indeed generate a much larger single-channel conductance, possibly as part of heterotetramers, or whether there is a regulatory influence in native cells, e.g., by an unknown effect of an accessory subunit. However, the generation of a >10 times larger conductance of an ion channel by a regulatory influence would be a new and singular mechanism indeed, at least to the best of our knowledge.

Gating of single HCN2 channels

Our recordings also show that both opening and closure of a single HCN2 channel proceed exclusively in single steps. This means that sublevel conductance states are not transiently adopted when a channel opens or closes. Hence, the typically slow activation time course of HCN2 channels is not caused by the individual gating of only one, two, or three subunits but by the concerted action of all four subunits. Therefore, models with one concerted opening step of all subunits, which is recruited differently depending on the degree of liganding, are adequate to describe the voltage-induced activation gating. In contrast, models with much larger complexity of the Koshland-Nemethy-Filmer (KNF) type (36) are not necessary. Considering this, the successful use of the MWC model (37) to describe the activation of HCN channels by voltage (15) is in agreement with our single-channel results. A model with only one concerted opening step has also been proposed for the ligand-induced gating of HCN2 channels (17) and related CNGA2 channels (38).

Our results also show that at saturating hyperpolarizing voltages, even in the absence of cAMP, the probability for a relevant closure of the channel is small once it has opened. In the presence of cAMP, this probability is further decreased, generating an open probability close to unity. We conclude from this that the activation time course of an HCN2 channel is given nearly solely by the first latency. Thus, the activation gating of an HCN channel is a very simple mechanism: Hyperpolarizing voltages switch the channel on to stay open, with only a few interruptions by closures.

cAMP enhances open probability

The enhancing and accelerating effect of cAMP on the macroscopic pacemaker current has been reported for different types of cells by applying cAMP, or 8-bromo-cAMP, or by stimulating the sympathetic signal-transduction cascade (39–42). Moreover, the effect has been confirmed for recombinant HCN2 channels (43–45).

For low-conductance HCN channels, as exclusively observed herein, the effect of cAMP on recordings with single-channel resolution has been reported so far only for native channels in sinoatrial node cells (19,29) and recombinant HCN2 channels (21). However, in those studies, the patches contained multiple channels and not only one channel, and therefore, the recordings did not allow for determination of whether the increase of channel activity by cAMP was caused by an increased open probability, P_o, of the same channels that were already active in the absence of cAMP or by an increased recruitment of further channels that were not active in the absence of cAMP. In contrast, we performed respective measurements in patches

containing one and only one channel. This allowed us to directly show that cAMP increases P_o of those channels that were already active in the absence of cAMP. This conclusion was based on the fact that in the absence of cAMP, P_o was sufficiently high to demonstrate that the patch indeed contained only one active channel.

HCN2 channels gate independently

The type of analysis we conducted to identify cooperativity in the activation process between neighbor channels was very simple and direct. We compared an averaged activation time course constructed from the activity of single channels in single-channel patches with activation time courses generated by multichannel patches (Fig. 6). If there is no interaction between the channels, the mean current of a multichannel patch is expected to follow a binomial distribution. This binomial distribution is determined at each time, t, by the open probability, $P_o(t)$, and the number of channels in the patch, N. When considering the 95% confidence interval of such a distribution along the averaged activation time course, the activation time courses arising from the multichannel patches did not deviate from the statistical prediction for independently gating channels. In other words, no cooperativity is required to explain the observed multichannel time courses.

Our result is in contrast to previous reports of HCN2 channels studied in multichannel patches obtained from HEK 293 cells, which provide evidence for a cooperative gating between neighbor channels (21). The reason for this difference is not clear. One explanation might be different experimental solutions. Although Dekker and Yellen (21) worked with symmetric solutions containing divalent Mg^{2+} ions, our solutions were Mg^{2+} free and contained Ca^{2+} ions only at the extracellular, not at the intracellular, side. Another explanation might be the different expression systems, HEK 293 cells versus *Xenopus* oocytes. Because the current density in the membrane of HEK 293 cells is certainly not higher than that of *Xenopus* oocytes, this would mean that more clusters of channels had formed in HEK293 cells than in *Xenopus* oocytes. High-resolution microscopic techniques might address this issue and also the question of whether or not there is a clustering of channels in native cardiac or neuronal cells. On the other hand, for analyzing the gating of an HCN2 channel from macroscopic currents by means of Markovian models (16,17), the oocyte expression system is appropriate, because independence of the channels can be assumed.

CONCLUSION

Single HCN2 ion channels open with a conductance of 1.67 pS, generate an open probability close to unity upon full activation, and work independently of their neighbor channels.

We are indebted to U. B. Kaupp for providing the mHCN2 cDNA. We also thank J. Kusch and V. Nache for helpful discussions, D.G.G. McMillan for critical reading of the manuscript, and K. Schoknecht, S. Bernhardt, and A. Kolchmeier for excellent technical assistance.

This work was supported by a grant from the Deutsche Forschungsgemeinschaft to K.B. and a Marie-Curie European Reintegration Grant to R.S.

REFERENCES

1. Biel, M., C. Wahl-Schott, …, X. Zong. 2009. Hyperpolarization-activated cation channels: from genes to function. *Physiol. Rev.* 89: 847–885.
2. Santoro, B., and G. R. Tibbs. 1999. The HCN gene family: molecular basis of the hyperpolarization-activated pacemaker channels. *Ann. N. Y. Acad. Sci.* 868:741–764.
3. Kaupp, U. B., and R. Seifert. 2001. Molecular diversity of pacemaker ion channels. *Annu. Rev. Physiol.* 63:235–257.
4. Ishii, T. M., M. Takano, and H. Ohmori. 2001. Determinants of activation kinetics in mammalian hyperpolarization-activated cation channels. *J. Physiol.* 537:93–100.
5. Santoro, B., S. Chen, …, S. A. Siegelbaum. 2000. Molecular and functional heterogeneity of hyperpolarization-activated pacemaker channels in the mouse CNS. *J. Neurosci.* 20:5264–5275.
6. Stieber, J., G. Stöckl, …, F. Hofmann. 2005. Functional expression of the human HCN3 channel. *J. Biol. Chem.* 280:34635–34643.
7. Chen, S., J. Wang, and S. A. Siegelbaum. 2001. Properties of hyperpolarization-activated pacemaker current defined by coassembly of HCN1 and HCN2 subunits and basal modulation by cyclic nucleotide. *J. Gen. Physiol.* 117:491–504.
8. Ulens, C., and J. Tytgat. 2001. Functional heteromerization of HCN1 and HCN2 pacemaker channels. *J. Biol. Chem.* 276:6069–6072.
9. Altomare, C., B. Terragni, …, D. DiFrancesco. 2003. Heteromeric HCN1–HCN4 channels: a comparison with native pacemaker channels from the rabbit sinoatrial node. *J. Physiol.* 549:347–359.
10. Er, F., R. Larbig, …, U. C. Hoppe. 2003. Dominant-negative suppression of HCN channels markedly reduces the native pacemaker current I(f) and undermines spontaneous beating of neonatal cardiomyocytes. *Circulation.* 107:485–489.
11. Wahl-Schott, C., and M. Biel. 2009. HCN channels: structure, cellular regulation and physiological function. *Cell. Mol. Life Sci.* 66:470–494.
12. Zagotta, W. N., N. B. Olivier, …, E. Gouaux. 2003. Structural basis for modulation and agonist specificity of HCN pacemaker channels. *Nature.* 425:200–205.
13. Lolicato, M., M. Nardini, …, A. Moroni. 2011. Tetramerization dynamics of C-terminal domain underlies isoform-specific cAMP gating in hyperpolarization-activated cyclic nucleotide-gated channels. *J. Biol. Chem.* 286:44811–44820.
14. Xu, X., Z. V. Vysotskaya, …, L. Zhou. 2010. Structural basis for the cAMP-dependent gating in the human HCN4 channel. *J. Biol. Chem.* 285:37082–37091.
15. Altomare, C., A. Bucchi, …, D. DiFrancesco. 2001. Integrated allosteric model of voltage gating of HCN channels. *J. Gen. Physiol.* 117:519–532.
16. Bruening-Wright, A., F. Elinder, and H. P. Larsson. 2007. Kinetic relationship between the voltage sensor and the activation gate in spHCN channels. *J. Gen. Physiol.* 130:71–81.
17. Kusch, J., S. Thon, …, K. Benndorf. 2012. How subunits cooperate in cAMP-induced activation of homotetrameric HCN2 channels. *Nat. Chem. Biol.* 8:162–169.
18. Kusch, J., C. Biskup, …, K. Benndorf. 2010. Interdependence of receptor activation and ligand binding in HCN2 pacemaker channels. *Neuron.* 67:75–85.
19. DiFrancesco, D. 1986. Characterization of single pacemaker channels in cardiac sino-atrial node cells. *Nature.* 324:470–473.

20. Kole, M. H., S. Hallermann, and G. J. Stuart. 2006. Single Ih channels in pyramidal neuron dendrites: properties, distribution, and impact on action potential output. *J. Neurosci.* 26:1677–1687.

21. Dekker, J. P., and G. Yellen. 2006. Cooperative gating between single HCN pacemaker channels. *J. Gen. Physiol.* 128:561–567.

22. Michels, G., F. Er, …, U. C. Hoppe. 2005. Single-channel properties support a potential contribution of hyperpolarization-activated cyclic nucleotide-gated channels and If to cardiac arrhythmias. *Circulation.* 111:399–404.

23. Simeone, T. A., J. M. Rho, and T. Z. Baram. 2005. Single channel properties of hyperpolarization-activated cation currents in acutely dissociated rat hippocampal neurones. *J. Physiol.* 568:371–380.

24. Bois, P., B. Renaudon, …, D. DiFrancesco. 1997. Activation of f-channels by cAMP analogues in macropatches from rabbit sino-atrial node myocytes. *J. Physiol.* 501:565–571.

25. Ludwig, A., X. Zong, …, M. Biel. 1998. A family of hyperpolarization-activated mammalian cation channels. *Nature.* 393:587–591.

26. Thibier, C., O. Mulner, and R. Ozon. 1982. In vitro effects of progesterone and estradiol-17 β on choleragen activated *Xenopus* oocyte adenylate cyclase. *J. Steroid Biochem.* 17:191–196.

27. Shin, K. S., B. S. Rothberg, and G. Yellen. 2001. Blocker state dependence and trapping in hyperpolarization-activated cation channels: evidence for an intracellular activation gate. *J. Gen. Physiol.* 117:91–101.

28. Rothberg, B. S., K. S. Shin, …, G. Yellen. 2002. Voltage-controlled gating at the intracellular entrance to a hyperpolarization-activated cation channel. *J. Gen. Physiol.* 119:83–91.

29. DiFrancesco, D., and M. Mangoni. 1994. Modulation of single hyperpolarization-activated channels (i(f)) by cAMP in the rabbit sino-atrial node. *J. Physiol.* 474:473–482.

30. Su, Z. C., W. H. Gao, …, L. Zhou. 2013. Counting of ion channels on a membrane patch aided by patch-clamp fluorometry. *Biophys. J.* 104:278a.

31. Michels, G., M. C. Brandt, …, U. C. Hoppe. 2008. Direct evidence for calcium conductance of hyperpolarization-activated cyclic nucleotide-gated channels and human native If at physiological calcium concentrations. *Cardiovasc. Res.* 78:466–475.

32. Brown, H. F., J. Kimura, …, A. Taupignon. 1984. The ionic currents underlying pacemaker activity in rabbit sino-atrial node: experimental results and computer simulations. *Proc. R. Soc. Lond. B Biol. Sci.* 222:329–347.

33. Denyer, J. C., and H. F. Brown. 1990. Pacemaking in rabbit isolated sino-atrial node cells during Cs^+ block of the hyperpolarization-activated current if. *J. Physiol.* 429:401–409.

34. Marshall, P. W., W. Rouse, …, B. J. McLoughlin. 1993. ICI D7288, a novel sinoatrial node modulator. *J. Cardiovasc. Pharmacol.* 21:902–906.

35. Harris, N. C., and A. Constanti. 1995. Mechanism of block by ZD 7288 of the hyperpolarization-activated inward rectifying current in guinea pig substantia nigra neurons in vitro. *J. Neurophysiol.* 74:2366–2378.

36. Koshland, Jr., D. E., G. Némethy, and D. Filmer. 1966. Comparison of experimental binding data and theoretical models in proteins containing subunits. *Biochemistry.* 5:365–385.

37. Monod, J., J. Wyman, and J. P. Changeux. 1965. On the nature of allosteric transitions: a plausible model. *J. Mol. Biol.* 12:88–118.

38. Biskup, C., J. Kusch, …, K. Benndorf. 2007. Relating ligand binding to activation gating in CNGA2 channels. *Nature.* 446:440–443.

39. Banks, M. I., R. A. Pearce, and P. H. Smith. 1993. Hyperpolarization-activated cation current (Ih) in neurons of the medial nucleus of the trapezoid body: voltage-clamp analysis and enhancement by norepinephrine and cAMP suggest a modulatory mechanism in the auditory brain stem. *J. Neurophysiol.* 70:1420–1432.

40. DiFrancesco, D., and P. Tortora. 1991. Direct activation of cardiac pacemaker channels by intracellular cyclic AMP. *Nature.* 351:145–147.

41. Larkman, P. M., and J. S. Kelly. 1997. Modulation of IH by 5-HT in neonatal rat motoneurones in vitro: mediation through a phosphorylation independent action of cAMP. *Neuropharmacology.* 36:721–733.

42. Pape, H. C., and D. A. McCormick. 1989. Noradrenaline and serotonin selectively modulate thalamic burst firing by enhancing a hyperpolarization-activated cation current. *Nature.* 340:715–718.

43. Moroni, A., A. Barbuti, …, D. DiFrancesco. 2000. Kinetic and ionic properties of the human HCN2 pacemaker channel. *Pflugers Arch.* 439:618–626.

44. Viscomi, C., C. Altomare, …, D. DiFrancesco. 2001. C terminus-mediated control of voltage and cAMP gating of hyperpolarization-activated cyclic nucleotide-gated channels. *J. Biol. Chem.* 276:29930–29934.

45. Wainger, B. J., M. DeGennaro, …, G. R. Tibbs. 2001. Molecular mechanism of cAMP modulation of HCN pacemaker channels. *Nature.* 411:805–810.